8-1-1998

A Low-Order Model for Vortex Shedding Patterns Behind Vibrating Flexible Cables

David J. Olinger
Worcester Polytechnic Institute, olinger@wpi.edu

A low-order model for vortex shedding patterns behind vibrating flexible cables

D. J. Olinger
Mechanical Engineering Department, Worcester Polytechnic Institute, Worcester, Massachusetts 01609

(Received 13 May 1997; accepted 8 April 1998)

A recent focus in studies of vortex shedding behind circular cylinders has been on the use of low-order dynamical systems such as circle maps to predict wake dynamics. These purely temporal models have been limited by their inability to describe three-dimensional spatial flow variations along the cylinder span, a hallmark of transitional flows such as the cylinder wake. In the present work this limitation is overcome through development of a spatial-temporal map lattice which utilizes a series of coupled circle map oscillators along the cylinder span. This model allows for the study of vortex shedding patterns and wake dynamics behind vibrating flexible cables. Required input for the model includes the forcing frequency, amplitude, mode shape, aspect ratio and wavelength of the cable, Reynolds number, vortex convection velocity, and various phase angles. Model output parameters studied in this work include vortex shedding patterns and wake response frequency. Standing wave mode shapes and traveling waves along the cable span are modeled. Lacelike vortex patterns are observed for the standing wave case. A physical mechanism for the lacelike patterns is postulated. For traveling waves oblique shedding patterns are confirmed. Nonharmonic forcing outside the classical lock-on region yields vortex dislocation patterns in the wake. Honeycomb patterns are also observed for higher-order mode shapes at large forcing amplitudes. The current work establishes a new class of models based on circle maps for modeling spatially varying cylinder wakes. © *1998 American Institute of Physics.* [S1070-6631(98)01108-8]

I. INTRODUCTION

In recent years the study of the nonlinear dynamics of wakes behind circular cylinders has been the focus of increased attention. For example, it has been shown that certain features of the wake of a rigid oscillating cylinder can be predicted by low-dimensional iterative models, such as the circle map.[1,2] The circle map,[3]

$$\theta_{n+1} = \theta_n + \Omega - \frac{K}{2\pi}\sin(2\pi\theta_n), \tag{1}$$

was used to study a cylinder wake subjected to an imposed oscillation of controlled amplitude and frequency. The circle map is a standard universal model describing systems with two coupled oscillators. The parameters in the circle map can be related to the wake situation as follows. The periodic vortex shedding from a stationary cylinder (at frequency f_{so}) and the imposed cylinder oscillation (at f_e) yield the unforced frequency ratio, $\Omega = f_{so}/f_e$. The parameter K is analogous to the imposed cylinder oscillation amplitude, A/D, where D is the cylinder diameter.

The circle map models the dynamics of the two nonlinearly coupled oscillators on a two-dimensional torus in phase space. The angular measure on a Poincaré section of this torus, θ_n, is obtained by strobing the two oscillator system at the forcing frequency f_e. The dynamics of the circle map are studied by determining the forced frequency ratio, $\omega = f_s/f_e = \lim_{n\to\infty}[(\theta_n - \theta_0)/n]$, where f_s is the vortex shedding frequency for the forced cylinder wake. Rational values of $\omega = p/q = f_s/f_e$, where p and q are integers, correspond to lock-on states at fractional ratios of the forcing frequency. Irrational ω values correspond to quasiperiodic states outside lock-on regions. Critical points for transition to chaos with universal properties have also been shown to exist.

New phenomena, such as multiple lock-on regions at fractional p/q ratios of the forcing frequency, were predicted in the cylinder wake (and later confirmed experimentally) using this perspective.[1,2] The wake was also shown to possess universal properties and circle map dynamics near critical points for the onset of chaos. Certain aspects of this approach have also been used to describe wake dynamics in other vortex shedding studies. Stansby[4] observed circle map dynamics (in the form of multiple lock-on regions) in forced cylinder wakes, although these findings were not interpreted from the dynamical system perspective, and instead were classified as an ''intermittent lock-on behavior.'' Circle map dynamics can also be identified in recent numerical and experimental studies.[5–9] In particular, Bernhardt *et al.*[9] have observed multiple lock-on regions at higher Reynolds number of 18 000 based on cylinder diameter.

Karniadakis and Triantafyllou[10] observed quasiperiodic and chaotic dynamics in a ''receptivity region'' near the lock-on region boundary using spectral methods. Karniadakis and Triantafyllou,[11] in a numerical study of the three-dimensional transitional wake, identified period-doubling phenomena in spanwise wake velocity signatures. Nakano and Rockwell,[12] in observations on a frequency-modulated cylinder wake, studied wake forcing near a critical golden mean point for the onset of chaos (without lock-on) to determine whether the coherence of the wake response

could be influenced. Lotfy and Rockwell[13] used ''phase clock'' concepts to interpret near wake structures from a blunt trailing edge subjected to controlled oscillations. Since the circle map (in the present context) is essentially a ''phase clock'' describing the phase of the vortex at the strobe frequency, f_e, comparisons between the present work and Lotfy and Rockwell may prove fruitful.

However, use of purely temporal dynamical systems, such as the circle map or period doubling scenarios, has been limited by their inability to describe spatial variations, a hallmark of transitional fluid flows such as the cylinder wake. In fact, a recent focus area is the study of spatial variations along the cylinder span particularly through flow visualization studies. Some of the three-dimensional phenomena that have been identified in stationary cylinder wakes include oblique and parallel shedding,[14] cellular shedding and vortex dislocations,[15–18] and small-scale three-dimensional instabilities (mode A–B) at higher transitional Reynolds numbers.[19,20] Recent findings have been summarized in Williamson.[21]

Three-dimensional wake structures behind vibrating cylinders or cables have been given less attention. Griffin and Ramberg[22] studied the wake behind a vibrating flexible cable, and proposed that the near wake at any point along the cable span could be sensibly represented by the near wake of a rigid cylinder vibrating under the same conditions of frequency, amplitude, and Reynolds number. Ramberg and Griffin[23] studied the effect of vortex coherence on flow-induced forces on vibrating cables. Triantafyllou[24] described the mechanisms giving rise to three-dimensional patterns in two-dimensional flows. One such mechanism involves the generation of three-dimensional wave patterns from a two-dimensional nonuniformity, such as spanwise variations in cylinder diameter. Nuzzi *et al.*[25] detailed the three-dimensional vortex formation from an oscillating cylinder with an imposed spanwise diameter nonuniformity.

Newman and Karniadakis[26–28] utilized a parallel spectral element Fourier method, developed by Henderson and Karniadakis,[29] to study flow over a flexible cable vibrations at laminar and transitional Reynolds numbers. This work quantified and compared the coupled cable-flow response for both forced and flow-induced cable vibrations. Newman and Karniadakis also identified two distinct vortex shedding responses, a ''lacelike'' structure for a standing wave cable shape, and an oblique shedding structure for traveling waves along the cylinder span.

The present work seeks to extend the use of low-order iterative models to spatially varying wake flows, such as the flow-induced vibration of a flexible cable. It overcomes the limitations of the previous temporal dynamical systems by developing a spatial-temporal model based on a series of coupled circle map oscillators placed along the cylinder span. This coupled map lattice is then used to predict vortex shedding patterns and wake dynamics behind a vibrating flexible cable with an externally imposed cable frequency, amplitude, and mode shape. This work comprises part of a larger effort to establish a dynamical systems framework to predict and organize vortex shedding phenomena in vibrating cylinder wakes.

Spatially coupled circle maps have been previously studied as models for high-dimensional chaos, with an emphasis on the resulting space–time dynamics and chaotic behavior. Alstrom and Ritala[30] studied mode locking in coupled circle maps with random phases and found very different behavior compared to a single circle map. Kaneko[31] investigated coupled map lattices as a model for spatiotemporal chaos and made some connections with Navier-Stokes equations. Kaneko[32] also has studied transitions among coherent, ordered, partially ordered and turbulent states in circle maps. Tsang *et al.*[33] studied globally coupled ordinary differential equations with application to Josephson junction arrays. The current work represents the first attempt to model wake flow dynamics directly with coupled circle maps.

The use of diffusively coupled oscillators along the cylinder span to model vortex shedding dynamics is not new. However, previous work has generally focused on the use of Ginzburg–Landau (GL)[34–37] or van der Pol equations[38,39] to model the wake dynamics, instead of the circle maps applied here. It is also interesting that coupled map lattices can model natural patterns as diverse as seashell patterns,[40] although these models have generally been heuristic or rule based. However, similarity of seashell and wake patterns (in the form of parallel, dislocation, and chevron structures) was a motivation for the present work by suggesting that a low-order dynamical system with universal features could model the similar patterns which occur in diverse physical systems.

The paper is organized as follows. In Sec. II the low-order model is developed. Section III details the method for determining vortex shedding patterns from the model. Section IV presents a summary of wake structures predicted by the coupled map lattice for various cable frequencies, vibration amplitudes, and standing wave mode shapes. Variation of oscillation frequency and amplitude is studied for both parallel and oblique shedding cases. The effect of traveling waves along the cylinder span and nonharmonic forcing are also studied. Comparison to previous experimental and numerical results is made, and a physical mechanism for lacelike structures in the standing wave case is postulated. Main results and future directions are summarized in Sec. V.

II. THE COUPLED MAP LATTICE

The key steps in development of a coupled map lattice (CML) include: (1) identifying the relevant physics in the flow; (2) modeling the spatial dynamics of each physical process by the simplest possible dynamics on the lattice; (3) numerically iterating the resultant CML in time; and (4) post-processing the CML iterates. In our model, a circle map is used to describe the interaction between the cable vibration and near wake vortex shedding, justified by the earlier success of the circle map in predicting wake dynamics.[1,2] We should also point out that earlier work[41] showed that a circle map could be developed using the Landau-Stuart equation[42,43] as a starting point. The Landau-Stuart equation can be deduced from the Navier-Stokes equations, and is also known to describe the wake evolution near the critical Reynolds number.[44,45] When an external forcing term is added to this equation, one can generate a coupled dynamical

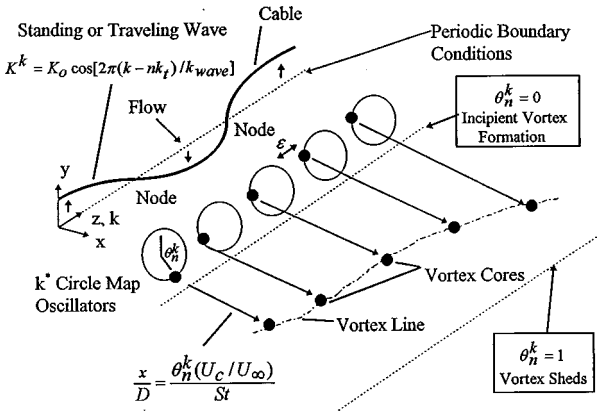

FIG. 1. Schematic of the coupled map lattice.

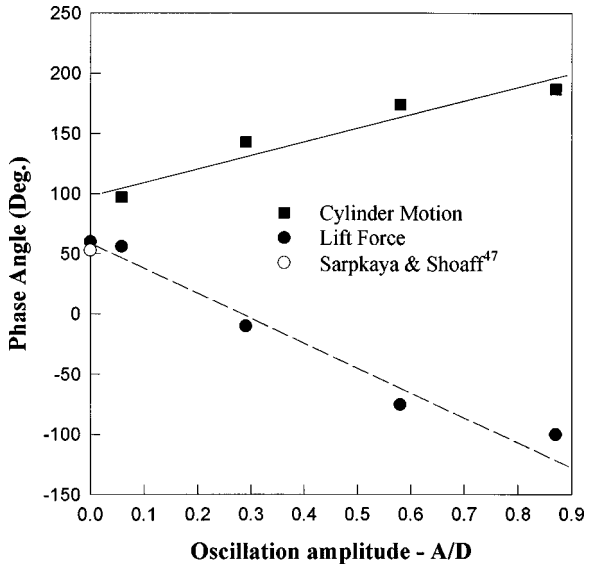

FIG. 2. Phase angle between the vortex shedding event and cylinder motion (or lift force) determined using a two-dimensional numerical Galerkin method.

system for the amplitude and phase of a disturbance in the forced wake. Numerical studies of this system exhibit circle map dynamics, and in the limit of low forcing, the system reduces directly to a circle map.[41]

Circle map oscillators are placed at established lattice points along the cable span as shown in Fig. 1, and coupled together with a simple diffusion model. This results in the coupled map lattice:

$$\theta_{n+1}^k = (1-2\varepsilon)F_n^k + \varepsilon(F_n^{k+1} + F_n^{k-1}), \tag{2}$$

$$F_n^k = \theta_n^k + \Omega - \frac{K^k}{2\pi}\sin\left[2\pi\theta_n^k - \phi_1^k - \frac{\pi}{2}\right], \tag{3}$$

where Eqs. (2) and (3) are a diffusion model and modified circle map, respectively. Here, k is an integer counter denoting the lattice site along the cable span. When modeling a wake flow with a circle map, the wake is effectively strobed at the cable oscillation frequency, f_e. As a result the wake dynamics are studied at discrete times $t = n\Delta t = n/2\pi f_e$ where n is an integer counter in time.

In the modified circle map θ_n^k represents the phase of the vortex shedding process at discrete time n and spanwise location k. θ_n^k varies between 0 and 1, i.e., modulo 1. Random initial conditions θ_0^k are used. The unforced frequency ratio $\Omega = f_{so}/f_e$ is defined as for the circle map, Eq. (1). The forcing term,

$$K^k = K_0 \cos[2\pi(k - nk_t)/k_{wave}], \tag{4}$$

models the cylinder oscillation amplitude along the cylinder. Both standing wave cable mode shapes ($k_t = 0$), and traveling waves along the cable ($k_t \neq 0$) can be specified. Here, k_t is the number of gridpoints which a traveling wave moves per forcing cycle, while k_{wave} is the imposed spatial wavelength of the standing wave. Rigid cylinders (K^k = constant) can also be modeled. Specification of input parameters Ω and K^k implies that a flexible cable with imposed external forcing, as opposed to a freely vibrating cable, is studied with the current model.

The input parameter ϕ_1^k represents the phase angle between the vortex shedding event and the cylinder motion at a given k location in a two-dimensional wake. The dependence of ϕ_1^k with cable vibration amplitude is presented in Fig. 2 from a classical Galerkin method applied to a two-dimensional cylinder flow.[46] Comparison with previous investigations[47] is shown. The phase angle ϕ_1^k models the shear layer from one side of the cylinder, with $\phi_2^k = \phi_1^k + \pi$ used for the second shear layer. The π phase shift is required to model the out-of-phase movement of the cable with respect to each individual shear layer. The CML treats the dynamics of the two shear layers independently with no shear layer interaction in the transverse direction. The $\pi/2$ phase angle in Eq. (3) places the forcing in-phase with the θ_n^k term (vortex shedding) if $\phi_1^k = 0$. This term is required due to the sine (as opposed to cosine) function in the forcing term.

The diffusion model, Eq. (2), is derived from a simple explicit finite difference technique applied to a diffusive partial differential equation (see the Appendix). The diffusion coefficient is given by

$$\varepsilon = \frac{\nu\Delta t}{(\Delta z)^2} = \frac{\Omega(k^*-1)^2}{2\pi\ \mathrm{St}\,\mathrm{Re}(AR)^2}, \tag{5}$$

where $\Delta t = (2\pi f_e)^{-1}$, $\mathrm{Re} = U_\infty D/\nu$, and the Roshko-Williamson relation,[14,48] $\mathrm{St} = (0.212\text{-}4.5/\mathrm{Re})/\cos\beta$ are used. Here, the input parameters k* and AR are the number of lattice points and cable aspect ratio, respectively.

Periodic-free boundary conditions are established with $\theta_n^{k*} = \theta_n^1$ to model parallel vortex shedding, for both forced and unforced (baseline) cases. To model oblique vortex shedding, periodic boundary conditions, $\theta_n^{k*} = \theta_n^1 + 1$, are established. This is justified since θ_n^k is treated modulo 1. While the linear diffusion model, Eq. (2), implies a trivial linear distribution of θ_n^k with k (i.e., oblique shedding) for the baseline oblique shedding case, our interest is in the response of this case to the imposed forcing. For the unforced oblique shedding case, the oblique shedding angle β is required as input, and $\mathrm{AR} = (U_c/U_\infty)/(\mathrm{St}\tan\beta)$, where $U_c/U_\infty = f(\mathrm{Re})$ is a nondimensional vortex convection velocity.[14] For this case, the diffusion coefficient is given by

$$\varepsilon = \frac{\nu \Delta t}{(\Delta z)^2} = \frac{\Omega (k^* - 1)^2 \mathrm{St} \tan^2 \beta}{2\pi \mathrm{Re} (U_c / U_\infty)^2}. \tag{6}$$

This expression is derived similar to Eq. (5), however, the two equations differ since we choose to express Eq. (6) in terms of the input parameters appropriate to the periodic boundary conditions for oblique shedding. Typically, $k^* = 100$ lattice sites, and 10^4 time iterations are used in the numerical iteration of the coupled map lattice, and the results represent the asymptotic dynamics.

III. VORTEX SHEDDING PATTERNS

The vortex shedding patterns presented in Sec. IV are developed by interpreting the phase of the vortex shedding process θ_n^k as follows (see Fig. 1). A value of $\theta_n^k = 0$ corresponds to incipient vortex formation (the start of the vortex formation process), while a value of $\theta_n^k = 1$ corresponds to the vortex shedding event (the start of the next shedding cycle). The phase of shedding θ_n^k is then transformed into a downstream vortex core location $(x/D)_n^k$ at every lattice point through

$$(x/D)_n^k = \theta_n^k x^* = \frac{\theta_n^k U_c}{\mathrm{St}\ U_\infty}, \tag{7}$$

since $x^* = (U_c / U_\infty)/\mathrm{St}$ yields a characteristic nondimensional vortex spacing in the streamwise direction.[14] This transformation implicitly identifies time with the streamwise direction. This is justified by the assumption that the vortex convection velocity is constant with downstream distance x/D,[14] i.e., uniformly traveling vortex structures.

The resultant wake structure is convected downstream without any additional diffusive coupling between adjacent lattice sites after the initial formation region in the near wake. The variation of the forced frequency ratio along the cable span can also be determined from $\omega^k = \mathrm{f}_\mathrm{s}^k / \mathrm{f}_\mathrm{e} = \lim_{n \to \infty} (\theta_n^k - \theta_0^k / n)$. A streamwise ''shift'' is applied to one shear layer with

$$(x/D)_n^{k\prime} = (x/D)_n^k \left[1 + \frac{2 - \omega^k}{2} \right], \tag{8}$$

where $(x/D)_n^{k\prime}$ is a corrected vortex core location. The term $(2 - \omega^k)/2$ derives from geometric considerations by noting the shift required to properly model the alternate vortex spacing in the natural shedding case (see Fig. 3) where $\omega^k = 1$, and $(2 - \omega^k)/2 = 1/2$. This shift is applied to the second shear layer for all cases in Sec. IV once ω^k is determined by the map. The model also accounts for shedding of more (or less) than one vortex core per forcing cycle.

IV. RESULTS AND DISCUSSION

In the following results, $\mathrm{Re} = 100$, to match the numerical simulations of Newman and Karniadakis.[26–28] In Fig. 3, typical vortex shedding patterns for parallel shedding along the cable span are presented. These show that the model can predict well-known parallel shedding phenomena behind a rigid circular cylinder (K^k=constant). Figure 3(a) shows the vortex shedding pattern resulting from the initial random θ_0^k distribution for the first few vortex shedding cycles. The shedding pattern evolves into parallel shedding in Fig. 3(b) after approximately 100 shedding cycles. Figure 3(a) and Fig. 3(b) are unforced shedding cases. In Fig. 3(c), the wake

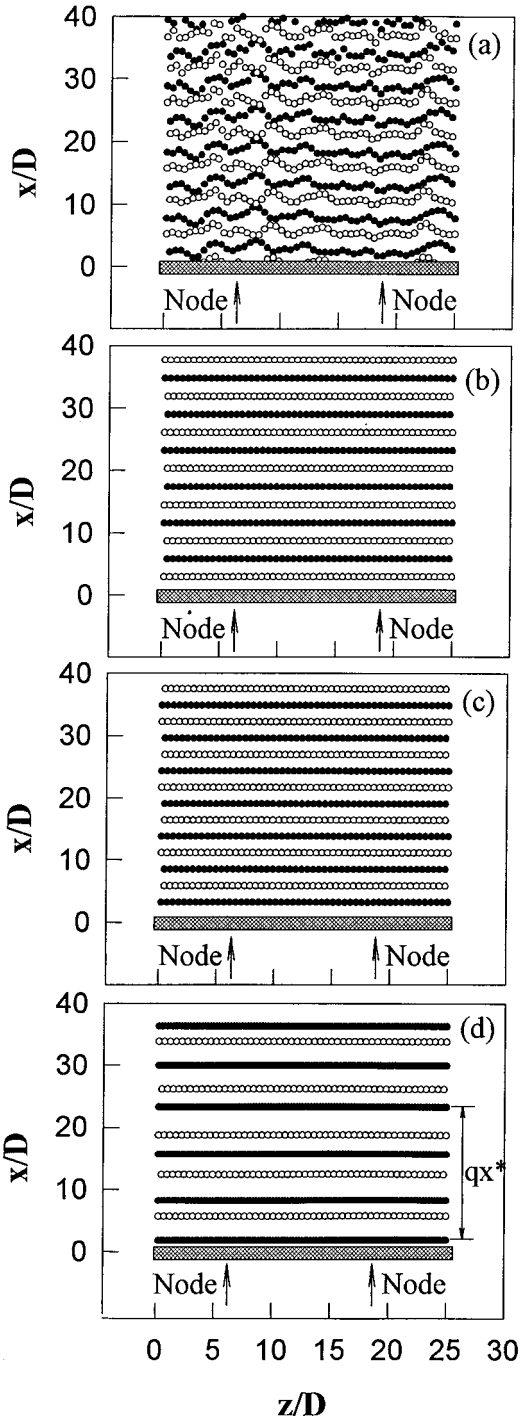

FIG. 3. Vortex shedding patterns for a rigid cylinder. (a) Initial random distribution of θ_0^k for unforced shedding case ($\mathrm{K}^k = 0$). After a sufficient number of shedding cycles the wake structure evolves to (b) the parallel shedding case for which $\Omega = \omega = 0.9$. (c) Lock-on state ($\Omega = 0.9$, $\mathrm{K}^k = 0.9$, $\omega = 1.0$). A shift in vortex spacing between (b) and (c) is observed. (d) A p/q=3/4 lock-on state ($\Omega = 0.725$, $\mathrm{K}^k = 0.9$, $\omega = 3/4$) with nonuniform vortex spacing. $k^* = 100$, AR=25, Re=100, $\mathrm{U_c}/\mathrm{U_\infty} = 0.88$ (from Ref. 14), periodic-free boundary conditions. Closed and open symbols represent vortex core locations for each shear layer, respectively.

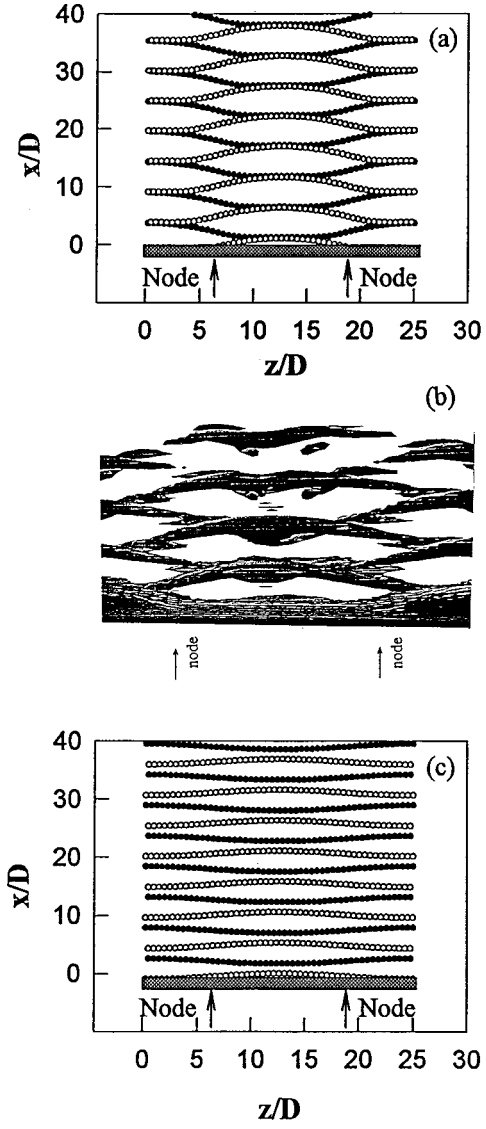

FIG. 4. (a) Lacelike structures for standing wave cable mode shapes from the coupled map lattice ($K_0=0.01$). (b) Iso-vorticity visualization from the numerical work of Newman and Karniadakis (Ref. 27) showing a lacelike structure. (c) ''Tuned'' lacelike structure ($K_0=0.0005$) from the coupled map lattice. In (a) and (c), $\Omega=1.0$, $k^*=100$, $k_{wave}=100$, A/D=0.68 at antinode (see Fig. 2), AR=25, Re=100, $U_c/U_\infty=0.88$, $\epsilon=0.15$, periodic-free boundary conditions.

is forced at $\Omega=0.9$, $K^k=0.9$ resulting in a lock-on state with $\omega=1.0$. The well-known shift in vortex spacing is observed between Fig. 3(b) and Fig. 3(c). Finally, in Fig. 3(d) wake structures near lock-on regions associated with fractional p/q ratios of the forcing frequency are studied. An $\omega=p/q=3/4$ lock-on case is presented with $\Omega=0.725$, $K^k=0.9$, and $\omega=3/4$. Nonuniform vortex spacing is observed between successive vortex lines in one shear layer. It is observed that p=3 vortices are shed during q=4 forcing cycles (corresponding to a downstream distance of qx*) consistent with the $\omega=p/q=3/4$ state.

In Fig. 4, a forced cable vibration within the lock-on region ($\Omega=1$, $K_0=0.01$) is studied. The vortex shedding pattern for a standing wave mode shape with nodes at z/D =6.25 and 18.75 (anti-nodes at z/D=0, 12.5, and 25) is presented. Here, the cable mode shape, aspect ratio AR=25, and cable amplitude A/D=0.68 (at an anti-node) are set to match the numerical simulations of Newman and Karniadakis.[26–28] Figure 4(a) shows a lacelike shedding pattern derived from the model. Iso-vorticity visualizations from Newman and Karniadakis's numerical work are shown in Fig. 4(b) for comparison. It is observed that the vortices shed simultaneously from the two shear layers near vibration anti-nodes, while alternate shedding occurs near vibration nodes. Newman and Karniadakis have confirmed this variation in wake structures along the cable span. The similar qualitative structure between the two cases implies that the coupled map lattice correctly models the phase between the shedding event and cable oscillation along the cylinder span. Comparison of Fig. 4(a) and Fig. 4(c) shows that the model can be ''tuned'' (through variation of K_0) to model vortex shedding patterns over a range of forcing amplitudes. We believe the modified lacelike structure of Fig. 4(c) should be observable in future experimental or numerical studies with large structural damping (i.e., lower oscillation amplitudes). Variation of the diffusion coefficient ϵ was found to have less of an effect on the resultant lacelike structure compared to K_0 variation.

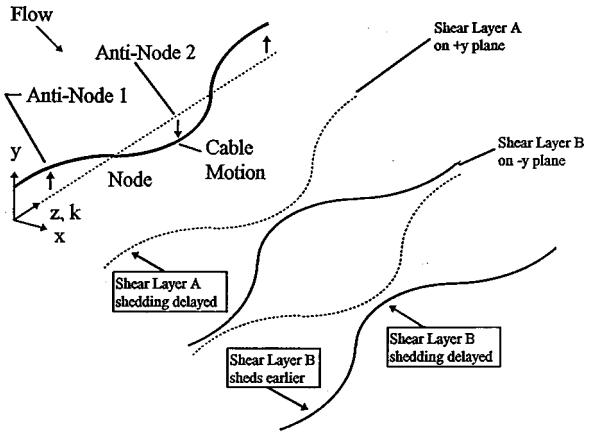

FIG. 5. Physical mechanism for lacelike vortex structures behind standing wave cable mode shapes.

We next briefly postulate a physical mechanism associated with the lacelike structures in Fig. 4. The lacelike structure arises due to the out-of-phase oscillation (modeled through the sinusoidal K^k term) of adjacent cable anti-nodes for the standing wave case. In Fig. 5 anti-nodes 1 and 2 oscillate 180° out-of-phase. Near anti-node 1, shedding of shear layer A is delayed due to movement of the cable *toward* the shear layer, while separation of the opposite shear layer B is enhanced. This separation enhancement (or inhibition) effect has been observed in Durgin *et al.*[49] Near anti-node 2 the opposite effect occurs, separation of shear layer A is enhanced, and shear layer B shedding delayed. When the flexible cable is 180° out-of-phase from the position shown in Fig. 5 (anti-node 1 at maximum negative *y* position), the cable induces the previously delayed vortices to shed.

Figure 6 studies the effect of nonharmonic forcing on the wake response (i.e., $\Omega=f_{so}/f_e\neq 1$). This type of forcing may have more dramatic effects on vortex shedding patterns for a

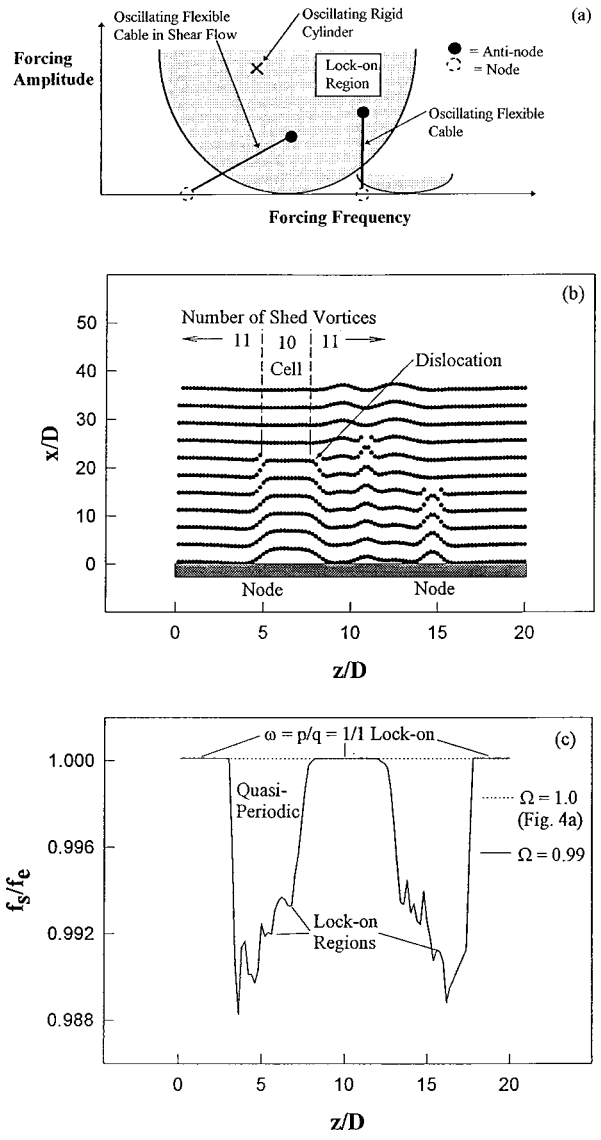

FIG. 6. (a) Forcing amplitude versus forcing frequency schematic showing that ranges in amplitude-frequency must be considered when interpreting oscillating cable results. For the oscillating flexible cable in a shear flow only one node and anti-node are shown. A W-shaped pattern is required if additional nodes (anti-nodes) are considered. (b) Vortex dislocation pattern for nonharmonic forcing case. One shear layer is shown. (c) Vortex shedding response frequency f_s/f_e vs z/D. $\Omega=0.99$, $K_0=0.10$, $k^*=100$, $k_{wave}=100$, A/D=0.68 at antinode, AR=20, Re=100, $U_c/U_\infty=0.88$, periodic-free boundary conditions.

flexible cable vibration, as opposed to rigid cylinder vibration, since for a standing wave vibration the cable vibration amplitude varies from zero (at nodes) to a maximum at the vibration anti-nodes. As a result, even for slight variations in Ω from 1.0, a portion of the cylinder span (near the nodes) will lie outside the lock-on region on a forcing amplitude-frequency diagram. This is shown in Fig. 6(a) where the nonharmonic oscillation of a flexible cable is represented by a vertical line. This figure points out that care must be taken in interpreting oscillating cable results. While oscillating rigid cylinder results can be interpreted using a single point on the amplitude-frequency diagram, cable results require a sequence of amplitude-frequency points to be considered.

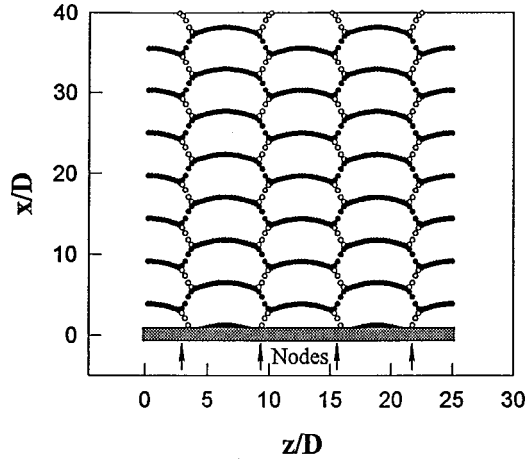

FIG. 7. Honeycomblike wake structure for higher-order mode shape at large forcing amplitude. $\Omega=1.0$, $K_0=1.2$, $k^*=100$, $k_{wave}=50$, A/D=0.68 at antinode, AR=25, Re=100, $U_c/U_\infty=0.88$, periodic-free boundary conditions. Simultaneous shedding occurs near cable anti-nodes.

This effect is confirmed in Fig. 6(b) where $\Omega=0.99$, and all other input parameters are set identical to Fig. 4(a). Vortex dislocations and lower frequency cells occur near the node locations. Figure 6(c) presents the variation in forced frequency ratio, $\omega=f_s/f_e$, along the cylinder span, showing that the model can predict vortex shedding response frequencies. Figure 6(c) shows that quasiperiodic states ($\omega\neq p/q$, $\omega\neq 1$) occur in the lower frequency cell near the node region, bracketed by lock-on regions ($\omega=1$). The wake structure adjusts to the alternating lock-on and quasiperiodic regions through formation of vortex dislocation structures. The association between quasiperiodic states and dislocations has been observed in studies of spanwise frequency cells in stationary cylinder flows.[14–16]

Interpreting these nonharmonic forcing results using the ampitude-frequency diagram of Fig. 6(a) suggests that additional lock-on states may occur along the cylinder span in addition to the $\omega=1$ lock-on regions near cable anti-nodes. The vertical line in Fig. 6(a) denoting this case passes through multiple lock-on regions[1,2] outside the primary one. These additional lock-on regions are observed and highlighted in Fig. 6(c). We have also plotted the wake response frequency from the standing wave case of Fig. 4(a) for comparison to the nonharmonic forcing. For the standing wave case, the vortex shedding frequency remains locked-on to the cable frequency across the entire span, consistent with results from Newman and Karniadakis's studies.

The effect of large amplitude forcing on the wake structure is studied in Fig. 7. Here, the intent is to study the chaotic regime ($K_0>1$) in the circle map. Figure 7 shows that the wake remains ordered within the lock-on region even at high forcing amplitudes. Disordered (chaotic) wake patterns are not observed, instead an interesting honeycomb pattern is observed for a higher-order mode shape ($k_{wave}=50$, $k^*=100$). Simultaneous shedding occurs near cable anti-nodes so that the vortex elements from both shear layers coincide. Some preliminary experimental evidence of honeycomb structures has been observed in higher-order mode cable vibrations.[50]

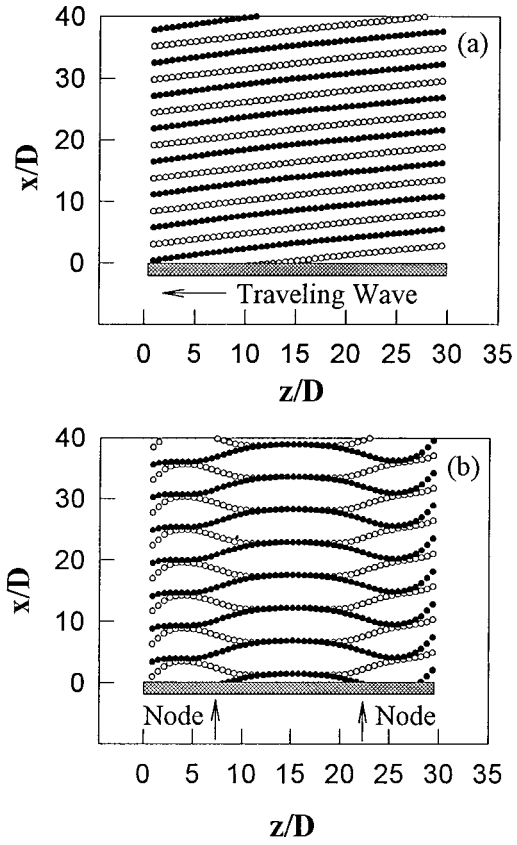

FIG. 8. Oblique shedding patterns for traveling wave along cable span. (a) Traveling wave case, (b) standing wave case. $\Omega=1.0$, $K_0=0.01$, $k^*=100$, $k_{wave}=100$, $A/D=0.68$ at antinode, $Re=100$, $U_c/U_\infty=0.88$, periodic boundary conditions, $\beta=10°$, $AR=(U_c/U_\infty)/(St\tan\beta)=30$.

In Fig. 8, the effect of traveling waves along the cable span on vortex shedding patterns is studied. Figure 8(a) shows the resultant oblique shedding for a traveling wave. The traveling wave retains a standing wave shape during its translation. The oblique shedding response associated with traveling waves has been observed by Newman and Karniadakis.[27] As in Ref. 27 the anti-nodes (and oblique wave front) travel across the full cable span during one shedding cycle due to the imposed periodic boundary conditions. The vortices are shed at the input oblique shedding angle $\beta=10°$, a typical oblique shedding angle from low Reynolds number experimental wake studies.[14,16]

The traveling wave case requires the periodic boundary conditions, $\theta_n^{k*}=\theta_n^1+1$, discussed in Sec. II. Figure 8(b) presents the vortex shedding pattern using this boundary condition for standing wave forcing ($k_t=0$). Some similarity with the lacelike structure of Fig. 4(a) is noted, however, a combined oblique/lacelike structure is observed here. Comparison of Figs. 8(a) and 8(b) shows that the oblique shedding pattern is determined by the traveling wave motion, and not solely a function of imposed boundary conditions.

V. CONCLUSIONS

Before presenting the main conclusions of this work, it is appropriate to summarize input information needed for the model, particularly those requiring experimental or numerical evidence. Input parameters include the frequency and amplitude of forcing, the number of lattice sites, and the free-stream Reynolds number. The vortex convection velocity, U_c/U_∞, and the Strouhal-Williamson relation for vortex shedding frequencies are input from experimental studies. The phase between the cylinder motion and the vortex shedding event as a function of cylinder oscillation amplitude for a two-dimensional wake flow (see Fig. 2) is determined from numerical studies. The cylinder aspect ratio and the spatial wavelength of the cable mode shape are required for the standing wave cases. The nondimensional cylinder oscillation amplitude at vibration anti-nodes is required as input for the flexible cable cases to utilize Fig. 2. Input of the traveling wave velocity and oblique shedding angle are required for traveling wave cases at the current stage of model development. Output parameters studied in this work include the vortex shedding patterns and wake response frequency ratio, f_s/f_e.

A low-order model based on a series of coupled circle map oscillators along the cylinder span has been developed. It is shown that this simple map can model vortex shedding patterns in the wake of forced flexible cables. Wake phenomena modeled include vortex dislocations, lacelike structures for standing wave cable shapes, oblique shedding for traveling waves along the cable span, and honeycomblike wake structures. These results establish a new class of low-order models for describing vortex shedding patterns in vibrating cylinder wakes, and are part of an ongoing effort to develop a circle map framework for organizing and predicting observed phenomena in spatially varying wake flows.

Before closing it is appropriate to discuss certain limitations of the present map. At the current state of development, the model is purely kinematic, and does not contain any dynamics such as hydrodynamic forces. Comparison with numerical simulations are largely qualitative, although quantitative agreement was found for wake response frequencies in a standing wave case, and anti-node travel velocities in oblique shedding cases. The present observations and these limitations lead naturally to the question: why does a fluid flow governed by coupled field equations follow the dynamics of a simple map? Our results imply that one should be able to extract the latter from the Navier-Stokes equations. Without this step, the connections implied can be viewed as unsatisfying. Some work[41] in this needed direction has already been described in Sec. II.

Future extensions to the model intended to overcome some of these limitations include: (1) study of free-stream shear flow effects on the vortex shedding patterns; (2) development of an iterative map, based on low-order harmonic oscillators, to model freely vibrating cables and hydrodynamic wake-cable coupling and forces; and (3) development of a two-dimensional vector map modeling streamwise and spanwise velocity dynamics for comparison to particle-image-velocimetry (PIV) visualizations. Preliminary results for the shear flow case suggest that combined standing wave-dislocation patterns[28] can be predicted by the model.

ACKNOWLEDGMENTS

This research has been supported by the Office of Naval Research (Grant No. N00014-96-1-0004) under the direction of Dr. Thomas Swean. The author wishes to G. E. Karniadakis for generously providing the visualization from his numerical studies. The experimental work of L. Meng, which led to increased understanding of the physical mechanism for lacelike structures, is gratefully acknowledged.

APPENDIX: DIFFUSION MODEL

The diffusion model, Eq. (2), is developed as follows. The diffusive vorticity transport equation:

$$\frac{\partial \omega}{\partial t} = -\mathbf{u}\cdot\nabla\omega + \omega\cdot\nabla\mathbf{u} + \nu\nabla^2\omega, \tag{A1}$$

where ω and $\mathbf{u}$ are the vorticity and velocity vectors, used as the starting point. Neglecting streamwise and transverse vorticity (ω_x, $\omega_y = 0$), streamwise and transverse variations in spanwise vorticity ($\partial\omega_z/\partial x = \partial\omega_z/\partial y = 0$), spanwise velocity variations ($\partial u/\partial z = \partial v/\partial z = \partial w/\partial z = 0$), and the spanwise velocity component ($w = 0$), yields

$$\frac{\partial w_z}{\partial t} = \nu\frac{\partial^2\omega_z}{\partial z^2}. \tag{A2}$$

Next, $\omega_z = \theta_n^k$, associating the parameter θ_n^k with the spanwise vorticity. This is justified from our earlier established correspondence between $\theta_n^k = 1$ and the vortex shedding event (Sec. III), where a critical level of spanwise vorticity is attained when the vortex sheds.

Application of a simple explicit finite difference technique to Eq. (A2) then results in,

$$\theta_{n+1}^k = (1-2\varepsilon)\,\theta_n^k + \varepsilon(\theta_n^{k+1} + \theta_n^{k-1}), \tag{A3}$$

where

$$\varepsilon = \frac{\nu\Delta t}{(\Delta z)^2}. \tag{A4}$$

The coupling between Eqs. (A3) and (3) requires $F_n^k = \theta_n^k$, and Eq. (2),

$$\theta_{n+1}^k = (1-2\varepsilon)F_n^k + \varepsilon(F_n^{k+1} + F_n^{k-1}) \tag{A5}$$

results.

[1] D.J. Olinger and K.R. Sreenivasan, ''Nonlinear dynamics of the wake of an oscillating cylinder,'' Phys. Rev. Lett. **60**, 797 (1988).
[2] D.J. Olinger and K.R. Sreenivasan, ''Universal dynamics in the wake of an oscillating cylinder at low Reynolds numbers,'' in *Proceedings of the ASME Symposium on Flow Induced Vibrations and Noise: Nonlinear Interaction Effects and Chaotic Motions*, edited by M. Reischman, M. Paidoussis, and R. Hansen (ASME, New York, 1988), Vol. 7, p. 1.
[3] S. Ostlund, D. Rand, J. Sethna, and E. Siggia, ''Universal properties of the transition from quasiperiodicity to chaos in dissipative systems,'' Physica D **8**, 303 (1983).
[4] P.K. Stansby, ''The locking-on of vortex shedding due to the cross-stream vibration of circular cylinders in uniform and shear flows,'' J. Fluid Mech. **74**, 641 (1976).
[5] A. Ongoren and D. Rockwell, ''Flow structure from an oscillating cylinder. Part 1: Mechanisms of phase shift and recovery in the near wake,'' J. Fluid Mech. **191**, 197 (1988).
[6] C. Barbi, D.P. Favier, C. A. Maresca, and D.P. Telionis, ''Vortex shedding and lock-on of a circular cylinder in oscillatory flow,'' J. Fluid Mech. **170**, 527 (1986).
[7] O.M. Griffin and M.S. Hall, ''Review - vortex shedding lock-on and flow control in bluff body wakes,'' Trans. ASME J. Fluids Eng. **113**, 526 (1991).
[8] B.E. Launder and M. Kato, ''Modeling flow-induced oscillations in turbulent flow around a square cylinder,'' *Proceedings of the ASME Forum on Unsteady Flows*, edited by W. Keith and T. Wei (ASME, Washington, D.C., 1993), Vol. 157, p. 189.
[9] J.E. Bernhardt, J. Mihailovic, C.F. Jines, A. Abouel-fotoh, T.C. Corke, and D.R. Williams, ''Instantaneous pressure distribution around an oscillating cylinder,'' APS Bulletin **41**, 1779 (1996).
[10] G. Karniadakis and G.S. Triantafyllou, ''Frequency selection and asymptotic states in laminar wakes,'' J. Fluid Mech. **199**, 441 (1989).
[11] G. Karniadakis and G.S. Triantafyllou, ''Three-dimensional dynamics and transition to turbulence in the wake of bluff objects,'' J. Fluid Mech. **238**, 1 (1992).
[12] M. Nakano and D. Rockwell, ''Flow structure in the frequency-modulated wake of a cylinder,'' J. Fluid Mech. **266**, 93 (1994).
[13] A. Lotfy and D. Rockwell, ''The near-wake of an oscillating trailing edge: mechanisms of periodic and aperiodic response,'' J. Fluid Mech. **251**, 173 (1993).
[14] C.H.K. Williamson, ''Oblique and parallel modes of vortex shedding in the wake of a circular cylinder at low Reynolds numbers,'' J. Fluid Mech. **206**, 579 (1989).
[15] D. Gerich and H. Eckelmann, ''Influence of end plates and free ends on the shedding frequency of circular cylinders,'' J. Fluid Mech. **122**, 109 (1982).
[16] H. Eisenlohr and H. Eckelmann, ''Vortex splitting and its consequences in the vortex street wake of cylinders at low Reynolds number,'' Phys. Fluids A **1**, 189 (1989).
[17] M. Koenig, H. Eisenlohr, and H. Eckelmann, ''Visualisation of the spanwise cellular structure of the laminar wake of wall-bounded circular cylinders,'' Phys. Fluids A **4**, 869 (1992).
[18] C.H.K. Williamson, ''The natural and forced formation of spot-like 'vortex dislocations' in the transition of a wake,'' J. Fluid Mech. **243**, 393 (1992).
[19] C.H.K. Williamson, ''The existence of two stages in the transition to three- dimensionality of a cylinder wake,'' Phys. Fluids **31**, 3165 (1988).
[20] C.H.K. Williamson, ''Three-dimensional wake transition,'' J. Fluid Mech. **328**, 345 (1996).
[21] C.H.K. Williamson, ''Vortex dynamics in the cylinder wake,'' Annu. Rev. Fluid Mech. **28**, 477 (1996).
[22] O.M. Griffin and S.E. Ramberg, ''The vortex-street wakes of vibrating cylinders,'' J. Fluid Mech. **66**, 553 (1974).
[23] S.E. Ramberg and O.M. Griffin, ''The effects of vortex coherence, spacing, and circulation on the flow-induced forces on vibrating cables and bluff structures,'' Naval Research Laboratory Report 7945 (1976).
[24] G.S. Triantafyllou, ''Three dimensional flow patterns in two-dimensional wakes,'' *Proceedings of the ASME Symposium on Unsteady Flows*, University of Toronto, Toronto, Canada, p. 395 (1990).
[25] F. Nuzzi, C. Magness, and D. Rockwell, ''Three-dimensional vortex formation from an oscillating, nonuniform cylinder,'' J. Fluid Mech. **238**, 31 (1992).
[26] D. Newman and G.E. Karniadakis, ''Flow structures in the wake of a flexible cable,'' *Proceedings of the 1995 Symposium on Fluid-Structure Interactions*, edited by T.C. Corke and D.R. Williams, 1995 ASME International Mechanical Engineering Congress & Exposition, San Francisco, CA, p. 55 (1995).
[27] D. Newman and G.E. Karniadakis, ''Simulations of flow over a flexible cable: A comparison of forced and flow-induced vibration,'' J. Fluids Struct. **10**, 43 (1996).
[28] D. Newman and G.E. Karniadakis, ''A direct numerical simulation of study of flow past a freely vibrating cable,'' J. Fluid Mech. **344**, 95 (1997).
[29] R.D. Henderson and G.E. Karniadakis, ''Unstructured spectral element methods for simulation of turbulent flows,'' J. Comput. Phys. **122**, 191 (1995).
[30] P. Alstrom and R. Ritala, ''Mode locking in an infinite set of coupled circle maps,'' Phys. Rev. A **35**, 300 (1987).
[31] K. Kaneko, ''Spatio-temporal chaos in one- and two-dimensional coupled map lattices,'' Physica D **37**, 60 (1989).
[32] K. Kaneko, ''Globally coupled circle maps,'' Physica D **54**, 5 (1991).
[33] K.Y. Tsang, R.E. Mirollo, S.H. Strogatz, and K. Wiesenfeld, ''Dynamics of a globally coupled oscillator array,'' Physica D **48**, 102 (1991).

[34]P. Albarède, M. Provansal, and L. Boyer, ''Modélisation par l'équation Ginzburg- Landau du sillage tridemnsionnel d'un obstacle allongé,'' C.R. Acad. Sci. Paris **310 (II)**, 459 (1990).
[35]P. Albarède and P.A. Monkewitz, ''A model for the formation of oblique shedding and 'chevron' patterns in cylinder wakes,'' Phys. Fluids A **4**, 744 (1992).
[36]P. Albarède and M. Provansal, ''Quasi-periodic cylinder wakes and the Ginzburg-Landau model,'' J. Fluid Mech. **291**, 191 (1995).
[37]P.A. Monkewitz, C.H.K. Williamson, and G.D. Miller, ''Phase dynamics of Karman vortices in cylinder wakes,'' Phys. Fluids **8**, 91 (1996).
[38]M. Gaster, ''Vortex shedding from slender cones at low Reynolds numbers,'' J. Fluid Mech. **38**, 565 (1969).
[39]B.R. Noack, F. Ohle, and H. Eckelmann, ''On cell formation of vortex streets,'' J. Fluid Mech. **227**, 293 (1991).
[40]C.H. Waddington and R.J. Cowe, ''Computer simulation of a molluscan pigmentation pattern,'' J. Theor. Biol. **25**, 219 (1969).
[41]D.J. Olinger, ''A low-dimensional model for chaos in open fluid flows,'' Phys. Fluids A **5**, 1947 (1993).
[42]L.D. Landau and E.M. Lifshitz, *Fluid Mechanics: Course in Theoretical Physics* (Pergamon, Oxford, 1959), Vol. 6, Chap. 3.
[43]J.T. Stuart, ''On the nonlinear mechanics of wave disturbances instable and ustable parallel flows. Part 1. The basic behaviour in plane Poiseuille flow,'' J. Fluid Mech. **9**, 353 (1960).
[44]M. Provensal, C. Mathis, and L. Boyer, ''Benard-von Karman instability: Transient and forced regimes,'' J. Fluid Mech. **182**, 1 (1987).
[45]K.R. Sreenivasan, P.J. Strykowski, and D.J. Olinger, ''Hopf bifurcation, Landau equations, and vortex shedding behind circular cylinders,'' *Proceedings of the Forum on Unsteady Flow Separation*, edited by K. N. Ghia (ASME Fluids Engineering Division, New York, 1987), Vol. 52, p. 1.
[46]D.J. Olinger, A.N. Alexandrou, and D.R. Keller, ''Non-harmonic forcing of a cylinder wake by a periodic freestream flow,'' *Proceedings of the 1995 Symposium on Fluid-Structure Interactions*, edited by T.C. Corke and D.R. Williams, 1995 ASME International Mechanical Engineering Congress & Exposition, San Francisco, CA, p. 41 (1995).
[47]T. Sarpkaya and R.L. Shoaff, ''Inviscid model of two-dimensional vortex shedding for transient and asymptotically steady separated flow over a cylinder,'' AIAA Paper No. 79-0281, 17th AIAA Aerospace Sciences Meeting, New Orleans (1979).
[48]A. Roshko, ''On the development of turbulent wakes from vortex street,'' NACA Rep. 1191 (1954).
[49]W.W. Durgin, P.A. March, and P.J. Lefebvre, ''Lower mode response of circular cylinders in cross-flow,'' J. Fluids Eng. **102**, 183 (1980).
[50]L.Meng, ''Flow visualization of vortex shedding from a freely vibrating flexible cable,'' M.S. Thesis, Worcester Polytechnic Institute, Worcester, MA, August 1996.